Stochastic Optimization for Combined Economic and Emission Dispatch with Renewables

[1]Mehdi Rahmani-andebili, *Student Member, IEEE* and [1,2]Ganesh K. Venayagamoorthy, *Senior Member, IEEE*
[1]Real-Time Power and Intelligent Systems Laboratory
The Holcombe Department of Electrical and Computer Engineering, Clemson University, SC 29634, USA
[2]Eskom Centre of Excellence in HVDC Engineering, University of KwaZulu-Natal, Durban, South Africa
mehdir@g.clemson.edu & gkumar@ieee.org

***Abstract*- Environmental issues of thermal power plants and depletion of natural energy resources are the main motivations for applying renewable energy sources (RESs) in power systems. Therefore, it is important to consider RESs when performing combined economic and emission dispatch (CEED). In this study, the variability and uncertainties concerned with RESs and load demand are addressed with batteries installed in the power system as energy storage systems and stochastic optimization applied to solve the problem. A case study is presented to demonstrate the economic and environmental benefits achieved as a result.**

NOMENCLATURE

A. Indices and Sets

$b \in S^B$	Battery
$l \in S^L$	Load
$g \in S^G$	Thermal plant
$pv \in S^{PV}$	Solar plant
$t \in S^T$	Time in minute
$w \in S^W$	Wind plant

B. System Parameters and Variables

$A^B(.)$	Effective ampere-hours throughput of battery
A^{B_Tot}	Total cumulative ampere-hours throughput of battery in its life cycle
$EC^G(.)$	Emission cost of thermal plant
$F(.)$	Time step objective function
$F^{FL}(.)$	Forward-looking objective function
$f^B(.)$	Cost function of battery
$f^G(.)$	Cost function of thermal plant
$FC^G(.)$	Fuel cost of thermal plant
$LLC^B(.)$	Battery life loss cost
$N\tau$	Number of time steps considered in forward-looking objective function
Nx	Number of uncertain states of system
$\underline{P^G}, \overline{P^G}$	Minimum and maximum power of thermal plant
$\overline{P^L}(.)$	Load demand
$P^G(.)$	Power of thermal plant
$P^W(.)$	Power of wind plant
$P^{PV}(.)$	Power of solar plant
$P^{B2G}(.)$	Power of battery while doing B2G
$P^{G2B}(.)$	Power of battery while doing G2B
$\underline{P^B}, \overline{P^B}$	Minimum and maximum power of battery
$Price^B$	Investment for purchasing a battery
RUR^G, RDR^G	Ramp up and ramp down rates of thermal plant
$\underline{SOC^B}, \overline{SOC^B}$	Minimum and maximum allowable state of charge of battery
$SWC^B(.)$	Battery switching cost
$x^f(.)$	Predicted value for uncertain state of system
$X^f(.)$	Set of predicted values for uncertain states of system
z_1^F, z_2^F, z_3^F	Fuel cost coefficients of thermal plant
z_1^E, z_2^E, z_3^E	Emission coefficients of thermal plant
γ^E	Emission cost factor
λ^B	Effective weighting factor concerned with life loss cost of battery
μ^{Err}	Mean of prediction errors
σ^{Err}	Standard deviation of prediction errors

C. SA Algorithm Parameters and Variables

N^{SA}	Number of trials for producing new solution at every stage
r^{SA}	Random value from a uniform distribution in range of [0,1]
$y^{SA}(.)$	Binary variable as indicator of acceptance of new solution
$p^{SA}(.)$	Adaptive probability for acceptance of new solution
μ^{SA}	Coefficient for gradually decreasing temperature of molten metal
$\varepsilon^{SA}(.)$	Internal energy of molten metal
$\theta^{SA}_{Initial}(.)$	Initial temperature of molten metal
$\theta^{SA}(.)$	Current temperature of molten metal

I. INTRODUCTION

Due to the critical environmental issues caused by burning fossil fuel in thermal power plants and emitting carbon into the atmosphere, emission levels of thermal plants should be considered in the generation scheduling problem. In other words, optimizing the problem of combined emission and economic dispatch (CEED) is a solution to address the above problem. The CEED problem is formulated by converting the emission level of thermal power plants into the emission cost functions and merging them into the economic dispatch problem [1]. In [2]-[3], the CEED problem considers ramp-rate limits of thermal power plants. Since renewable energy source (RESs) technologies are developing rapidly and receive increasing attention [4], their presence must be considered in the economic dispatch problem. Installing RESs in power

This work is supported in part by the US National Science Foundation (NSF) under grants #1312260, #1308192 and #1232070 and the Duke Energy Distinguished Professor Endowment Fund. Any opinions, findings and conclusions or recommendations expressed in this material are those of the author(s) and do not necessarily reflect the views of National Science Foundation and Duke Energy.

978-1-4799-7560-0/15 $31.00 © 2015 IEEE
DOI 10.1109/SSCI.2015.179

system that convert the CEED problem into the CEED-RESs problem can mitigate energy security and environmental issues of power generation system. However, due to dependency of output power of RESs to the intermittent natural energy resources, RESs generation is variable and there is a high uncertainty about it. In [5], the impact of variability and uncertainty at multiple operational timescales has been studied. Also, the effects of solar power variability and forecast uncertainty on power system operation in the Arizona Public Service system has been studied in [6].

The CEED-RESs problem cannot be solved with deterministic methods, since the problem involves uncertainties. In [7], the economic dispatch problem in the presence of RESs has been studied probabilistically considering wind speed, solar irradiance and load demand as random variables and applying non-linear constrained optimization methods. In [8], a probabilistic method has been applied to solve the economic dispatch problem which considers the uncertainties of the generators reliability and wind power using corresponding probability distribution function. In [9], the economic dispatch problem which considers wind power has been solved by an expectation model assuming that the wind speed distribution satisfies the Weibull distribution function. In [10], the authors have applied best-fit participation factor methods in the economic dispatch problem which considers variability of RESs power and load demand. However, in the above mentioned studies, probability distribution functions have been assumed as the models for inherently unpredictable generation level of RESs or they have been applied to address the uncertainties of the predicted data. In addition, the environmental aspect of thermal power plants has not been considered.

Cost and emission reductions in a smart grid by maximum utilization of plug-in electric vehicles and RESs are presented in [11]. Particle swarm optimization is utilized to solve the stochastic optimization problem. A stochastic optimization technique is also presented and applied to solve the CEED-RESs problem in this paper. In this methodology, the uncertain states of the system are forecasted and their uncertainties are addressed by applying scenario-based approaches and solving the problem stochastically. Herein, the problem is optimized minute by minute to increase accuracy of the predicted data and decrease the range of uncertainties in the system states.

The rest of the paper is outlined as follows. In Section II, the CEED-RESs problem is formulated. The proposed methodology is introduced and described in Section III. Numerical studies carried out are explained in Section IV. Finally, the conclusion is given in Section V.

II. CEED-RESs Problem

A. Objective Function

The objective function of the CEED-RESs problem comprises two types of cost functions that involve a set of batteries as the energy storage systems and a set of thermal power plants. Herein, generation level of every battery and generation level of every power plant are considered as the variables of the CEED-RESs problem.

$$F(t) = \sum_{g \in S^G} f_g^G(\mathrm{t}) + \sum_{b \in S^B} f_b^B(\mathrm{t}) \qquad (1)$$

$$\forall t \in S^T, S^T = \{1, \cdots, Nt\}, S^G = \{1, \cdots, Ng\}, S^B = \{1, \cdots, Nb\}$$

1) Batteries' cost function

As can be seen in (2), the cost function of a battery includes life loss cost and switching cost.

$$f_b^B(\mathrm{t}) = LLC_b^B(t) + SWC_b^B(t), \forall t \in S^T, \forall b \in S^B \qquad (2)$$

The value of life loss cost of every battery is determined based on the effective ampere-hours throughput of the battery (A^B) due to the battery-to-grid (B2G) and grid-to-battery (G2B) actions, as can be seen in (3) [12]. Herein, A^{B_Tot} is the total cumulative ampere-hours throughput of the battery in its life cycle, $Price^B$ is the price of a battery, and value of λ^B, as the effective weighting factor, is determined using the introduced model in [12]. In the presented model, value of the effective weighting factor has a nonlinear relationship with the state of charge (SOC) of the battery.

$$LLC_b^B(t) = \frac{\lambda^B \times A_b^B(t)}{A_b^{B\_Tot}} \times Price_b^B, \forall t \in S^T, \forall b \in S^B \qquad (3)$$

Moreover, value of the switching cost of every battery is calculated using (4). This value of cost is considered whenever the battery is changed from the generation state to the load state or vice versa. In fact, this cost term prevent the battery from unnecessary switching that is harmful to its life cycle.

$$SWC_b^B(t) = \frac{10}{A_b^{B\_Tot}} \times Price_b^B \qquad (4)$$
$$\forall t \in S^T, \forall b \in S^B$$

2) Thermal power plants' cost function

The cost function of a thermal power plant includes fuel cost and emission cost presented in (5).

$$f_g^G(\mathrm{t}) = FC_g^G(t) + EC_g^G(t), \forall t \in S^T, \forall g \in S^G \qquad (5)$$

The fuel cost and emission cost of every thermal power plant are considered quadratic polynomials presented in (6) and (7), respectively.

$$FC_g^G(t) = z_{1,g}^F \times \left(P_g^G(t)\right)^2 + z_{2,g}^F \times \left(P_g^G(t)\right) + z_{3,g}^F \qquad (6)$$
$$\forall t \in S^T, \forall g \in S^G$$

$$EC_g^G(t) = \gamma^E \times \left(z_{1,g}^E \times \left(P_g^G(t)\right)^2 + z_{2,g}^E \times \left(P_g^G(t)\right) + z_{3,g}^E\right), \forall t \in S^T, \forall g \in S^G \qquad (7)$$

B. Constraints

In the following the constraints of the problem that must be held at every time step of the operation period are presented.

1) System power balance limit

Herein, power of every battery is considered positive if the battery is doing B2G and this power is supposed to be negative if the battery is doing G2B.

$$\sum_{g\in S^G} P_g^G(t) + \sum_{w\in S^W} P_w^W(t) + \sum_{pv\in S^{PV}} P_{pv}^{PV}(t) + \sum_{b\in S^B} P_b^B(t) = \sum_{l\in S^L} P_l^L(t), \forall t \in S^T \quad (8)$$

$$S^L = \{1,\cdots,Nl\}, S^W = \{1,\cdots,Nw\}, S^{PV} = \{1,\cdots,Npv\}$$

2) Thermal power plants' power limits

The maximum power and minimum power constraints of every thermal power plant is presented in (9).

$$\underline{P_g^G} \le P_g(t) \le \overline{P_g^G}, \forall t \in S^T, \forall g \in S^G \quad (9)$$

3) Thermal power plants' ramp up/down rates limits

The ramp-up rate and ramp-down rate constraints of every thermal power plant are presented in (10) and (11), respectively.

$$\left(P_g^G(t+1) - P_g^G(t)\right) \le RUR_g^G \quad \forall t \in S^T, \forall g \in S^G \quad (10)$$

$$\left(P_g^G(t) - P_g^G(t+1)\right) \le RDR_g^G \quad \forall t \in S^T, \forall g \in S^G \quad (11)$$

4) Batteries' power limits

As can be seen in (12), every battery can act as a load or generator by doing G2B and B2G, respectively. The output and input power limits of every battery in B2G and G2B operations are presented in (13) and (14), respectively.

$$P_b^B(t) = \begin{cases} P_b^{B2G}(t), & P_b^B(t) > 0 \\ P_b^{G2B}(t), & P_b^B(t) < 0 \end{cases}, \forall t \in S^T, \forall b \in S^B \quad (12)$$

$$\underline{P_b^B} \le P_b^{B2G}(t) \le \overline{P_b^B}, \forall t \in S^T, \forall b \in S^B \quad (13)$$

$$-\overline{P_b^B} \le P_b^{G2B}(t) \le -\underline{P_b^B}, \forall t \in S^T, \forall b \in S^B \quad (14)$$

5) Batteries' state of charge limits

In order to prolong the lifetime of the batteries, every battery must not be discharged more than the allowable depth of discharge (DOD). Moreover, every battery may have an upper limit for its SOC. Thus, the allowable limits for SOC of every battery are as (15).

$$\underline{SOC_b^B} \le SOC_b^B(t) \le \overline{SOC_b^B}, \forall t \in S^T, \forall b \in S^B \quad (15)$$

III. Proposed Methodology

As can be seen in Fig. 1, based on the proposed methodology that demonstrates its adaptability and dynamic characteristic, at every time step, the problem is solved for the updated optimization time horizon $(t+1,\cdots,t+N\tau)$; however, just dispatch signals of the next time step $(t+1)$ are accepted as the decision signals. Therefore, the objective function of the problem can be defined as (16), which is a forward-looking objective function. As can be seen, the forward-looking objective function is the sum of the time step objective functions over the optimization time horizon.

$$F^{FL}(t) = \sum_{\tau=1}^{N\tau} F(t+\tau), \forall t \in S^T \quad (16)$$

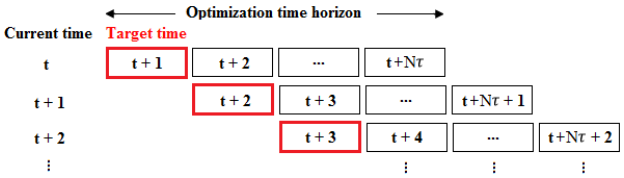

Fig. 1. Concept of the proposed adaptive and dynamic optimization technique.

A flowchart of the proposed methodology that uses simulated annealing (SA) algorithm as its optimization tool is illustrated in Fig. 2. As can be seen, at first, the system parameters along with the forecasted system states are received. Then, uncertainties of the predicted data are modeled using a scenario-based approach. After that, the problem is optimized stochastically by a SA algorithm. Next, values of the problem variables just for the next time step are accepted as the decision signals. This process is repeated for every time step (minute) of a day over the operation period $(1,\cdots,1440)$.

A. Forecasting uncertain states of the system

In this study, values of wind speed (v^W), solar irradiance (ρ^{PV}), and load demand (P^L) as the uncertain states of the system are predicted for the next $N\tau$ time steps using a neural network trained with Levenberg-Marquardt back-propagation algorithm that exist in MATLAB. A set of the forecasted values for the system's uncertain states over the next $N\tau$ time steps is presented in (17).

$$X^f(t) = \begin{Bmatrix} x_1^f(t) & \cdots & x_{Nx}^f(t) \\ \vdots & \cdots & \vdots \\ x_1^f(t+N\tau) & \cdots & x_{Nx}^f(t+N\tau) \end{Bmatrix} \quad (17)$$

$$\forall t \in S^T, x \in \{v^W, \rho^{PV}, P^L\}, Nx = Nw + Npv + Nl$$

In the following, the output power of wind and solar plants are determined using the functions presented in [13]-[14].

1) Wind power plant

The output power of a wind power plant has a nonlinear relationship with wind speed presented in (18) [13].

$$P_w^W(t) = \begin{cases} 0 & v_w^{W\_f}(t) < v_w^{ci}, v_w^{co} < v_w^{W\_f}(t) \\ P_w^{W\_r} \times \dfrac{v_w^{W\_f}(t) - v_w^{ci}}{v_w^r - v_w^{ci}} & v_w^{ci} \le v_w^{W\_f}(t) \le v_w^r \\ P_w^{W\_r} & v_w^r \le v_w^{W\_f}(t) \le v_w^{co} \end{cases} \quad (18)$$

$$\forall t \in S^T, \forall w \in S^W$$

Where $v_w^{W\_f}(.)$ is the forecasted value for the wind speed (m/s), v_w^{ci} is the cut-in wind speed (m/s), v_w^r is the rated wind speed (m/s), v_w^{co} is the cut-out wind speed (m/s), and $P_w^{W\_r}$ is the rated output power of the wind power plant (MW).

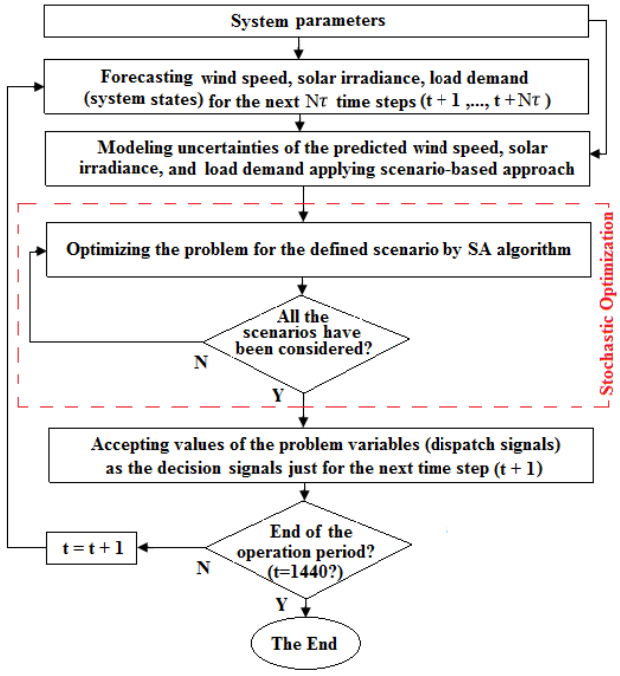

Fig. 2. Flowchart of the proposed methodology.

2) Solar power plant

The output power of a solar power plant is given as a function of solar irradiance presented in (19) [14].

$$P_{pv}^{PV}(t) = \begin{cases} P_{pv}^{PV\_r} \times \dfrac{\left(\rho_{pv}^{PV\_f}(t)\right)^2}{\rho_{pv}^{st} \times \rho_{pv}^{0}} & 0 \le \rho_{pv}^{PV\_f}(t) \le \rho_{pv}^{0} \\ P_{pv}^{PV\_r} \times \dfrac{\rho_{pv}^{PV\_f}(t)}{\rho_{pv}^{st}} & \rho_{pv}^{PV\_f}(t) > \rho_{pv}^{0} \end{cases} \quad (19)$$
$$\forall t \in S^{T}, \forall pv \in S^{PV}$$

Where $\rho_{pv}^{PV\_f}(.)$ is the forecasted value for the solar irradiance (W/m^2), ρ_{pv}^{st} is the solar irradiation in the standard environment set as 1000 W/m^2, ρ_{pv}^{0} is a certain irradiation point set as 150 W/m^2, $P_{pv}^{PV\_r}$ is rated output power of the solar power plant (MW).

B. Modeling uncertainties of the forecasted data

In this study, in order to address the uncertainties of the predicted data, a scenario-based approach is applied [15]. Herein, in the validation and testing processes of the data forecasting, the output data is compared with the target data and values of prediction errors are measured (Fig. 3 (a)). Then they are fitted on an appropriate probability density function curve (Fig. 3 (b)). Herein, it was observed that the predication errors can be fitted precisely on a Gaussian probability density function with an appropriate mean (μ^{Err}) and standard deviation (σ^{Err}). After that, the curve is divided into three areas to define three distinct values for the prediction inaccuracy with the probabilities about 0.1587, 0.6826 and 0.1587 related to $\mu^{Err} - 2\sigma^{Err}$, μ^{Err}, and $\mu^{Err} + 2\sigma^{Err}$, respectively. Therefore, at every time step, each uncertain state of the system has three different values with different probabilities. Based on this concept, several effective scenarios are defined for the values of every uncertain state of the system over the optimization time horizon, which are graphically illustrated in Fig. 4.

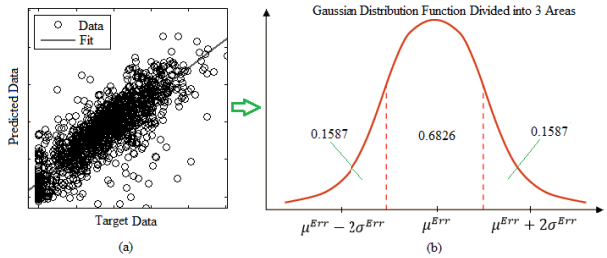

Fig. 3. (a): Prediction errors by comparing value of difference between target and output data, (b): Gaussian probability density function related to the fitted prediction errors of an uncertain state of the system.

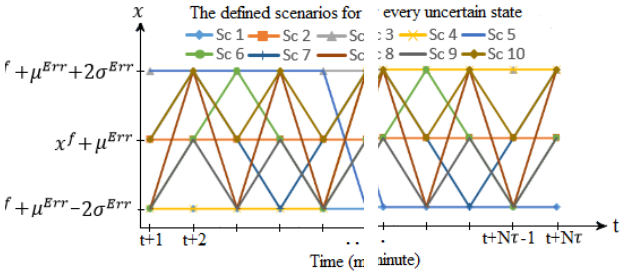

Fig. 4. The defined scenarios for value of every uncertain state of the system over the optimization time horizon.

C. SA algorithm as the optimization tool

In this study, SA algorithm is applied to solve the optimization problem. Other optimization algorithms could be used in this problem such as particle swarm optimization.. Herein, value of the forward-looking objective function is defined as the value of internal energy of molten metal (ε^{SA}) and then it is used to minimize the value of this energy. In the following, different steps for applying SA algorithm are presented and described.

Step 1: *Primary data*

Setting controlling parameters of the SA algorithm: These parameters include $\theta_{Initial}^{SA}$, N^{SA}, and μ^{SA}.

Parameters of the system: Values of all the system parameters and the predicted states of the system which considers their uncertainties included in the defined scenario are obtained.

Initial solution: A random solution for the problem variables is generated as an initial solution.

Step 2: *Generating an acceptable solution*

Generating new solution: A random solution for the problem variables is generated in the vicinity of the old one.

Checking problem constraints: All the problem constraints are checked for the optimization time horizon and if they are correct, the value of the internal energy of the molten metal is measured and the next step is executed, otherwise, the process is repeated form Step 2.

Checking SA acceptance criterion: The SA acceptance criterion is presented in (20). Based on this principle, a problem solution results in decreased internal energy of the molten metal. This is always accepted; however, the solution with increased value of the internal energy is accepted just by

an adaptive probability presented in (21). The value of this adaptive probability is decreased as the molten metal is cooled.

$$y_k^{SA}(t)=\begin{cases}1 & \varepsilon_{k+1}^{SA}(t)<\varepsilon_k^{SA}(t)\\ 1 & \varepsilon_{k+1}^{SA}(t)\geq\varepsilon_k^{SA}(t),\ \ r_k^{SA}>p_k^{SA}(t)\\ 0 & \varepsilon_{k+1}^{SA}(t)\geq\varepsilon_k^{SA}(t),\ \ r_k^{SA}\leq p_k^{SA}(t)\end{cases} \quad (20)$$

$$\forall t\in S^T,\forall k\in S^K, S^K=\{1,\cdots,Nk\}$$

$$p_k^{SA}(t)=e^{-\frac{\varepsilon_{k+1}^{SA}(t)-\varepsilon_k^{SA}(t)}{\theta_k^{SA}(t)}},\forall t\in S^T,\forall k\in S^K \quad (21)$$

Step 3: *Checking number of iteration for the current temperature*

If the number of iterations in the current temperature are not equal to the predefined value (N^{SA}), the process is repeated from Step 2, otherwise, temperature of the molten metal is decreased based on (22).

$$\theta_{k+1}^{SA}(t)=\mu^{SA}\times\theta_k^{SA}(t),\forall t\in S^T,\forall k\in S^K \quad (22)$$

Step 4: *Concluding*

Checking temperature of the molten metal: Temperature of the molten metal is measured and if the molten metal is frozen, the optimization process is finished, otherwise, the process is repeated from Step 2.

Introducing outcomes: The consequences include optimal values for the problem variables.

IV. Numerical Studies

A. Initial Data

Fig. 5 illustrates the configuration of the system under a study that includes wind and solar power plants, batteries as the energy storage system, and thermal power plants. The technical data of the thermal power plants includes their fuel cost coefficients, emission coefficients, and power limits are presented in Table I. Herein, values of ramp-up and ramp-down rates of all the thermal power plants are considered about 50 MW/min. Moreover, the thermal power plants are considered to be steam-electric plants [16]. Also, the type of the fuel consumed by the plants 1-4 and 7 (at buses 2, 3, 13, 19 and 27) are considered to be natural gas and types of the fuels consumed by the plant 5 and plant 6 (at buses 22 and 23) are considered sub-bituminous and residual oil (No. 6), respectively [16]. The amount of emission in Lbs/kW^{2}h released by a typical steam-electric plant for different types of the fuel have been presented in [16]. Furthermore, the value of penalty for emission is assumed about $10 per ton based on the California Air Resources Board auction of greenhouse gas emissions [17].

The rated output power of the wind and solar power plants are 40 and 20 MW, respectively. The rated power and capacity of every battery is assumed to be about 40 MW and 200 MWh, respectively. The minimum and maximum operational powers of every battery are considered about 5 MW and 40 MW, respectively. Moreover, the minimum and maximum allowable limits for SOC of every battery are considered about 30% and 100%, respectively. Herein, every battery has an initial SOC about 50%. The value of investment for purchasing a battery, and also value of total cumulative ampere-hours throughput of every battery in its life cycle are considered about $1,000,000 and 1000,000 ampere-hours, respectively. Moreover, the system voltage level 400 kV.

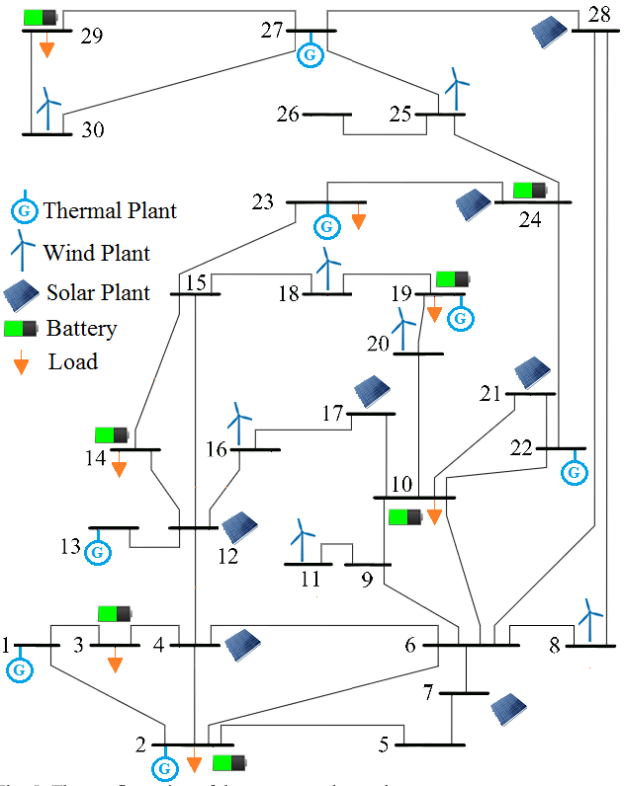

Fig. 5. The configuration of the system under study.

TABLE I
TECHNICAL DATA OF THE THERMAL POWER PLANTS

Plant	1	2	3	4	5	6	7
$\alpha_{1,g}^F$ ($/MW^{2}h)	0.690	0.689	0.689	0.899	0.913	0.992	0.983
$\alpha_{2,g}^F$ ($/MWh)	16.50	19.70	22.26	27.74	25.92	27.27	27.79
$\alpha_{3,g}^F$ ($)	680	450	370	480	660	665	670
$\alpha_{1,g}^E$ (Lbs/kW^{2}h)	0.122	0.122	0.122	0.122	0.216	0.181	0.122
$\alpha_{2,g}^E$ (Lbs/kWh)	1.220	1.220	1.220	1.220	2.160	1.810	1.220
P_g^G (MW)	20	15	10	20	10	10	10
$\overline{P_g^G}$ (MW)	180	180	180	150	150	150	150

Herein, the operation period and the optimization time horizon used in the forward-looking objective functions are considered 1440 minutes and 10 minutes, respectively. Moreover, in all the simulations, every time that SA algorithm is executed, values of its controlling parameters include $\theta_{initial}^{SA}$, N^{SA}, and μ^{SA} are set about 100 centigrade, 90 times, and 0.8, respectively. The forecasted demand levels at different system buses are presented in Fig. 6. Also, Fig. 7 illustrates the forecasted power of wind and solar power plants installed at bus 4 and 8.

B. Problem Simulations

Optimizing the CEED-RESs problem and considering RESs as the negative load results in about $2,452,900/day as the

total operation cost and around 99,023 ton/day as the total emission of the system. The generation levels of the thermal power plants that have noticeable fluctuations are shown in Fig. 8.

After optimizing the CEED-RESs problem with the proposed technique, the results are $2,291,700/day and 89,859 tons/day as the total operation cost and total emissions of the system, respectively. Herein, the value of savings for cost and emission are $161,200/day and 9,164 tons/day, respectively. Fig. 9 illustrates generation levels of the thermal power plants. As can be observed, generation variability of the thermal plants has been decreased considerably compared with the results presented in Fig. 8. Moreover, Fig. 10 demonstrates generation levels and SOC of every battery for every minute of the operation period. As can be seen, the SOC level is changed throughout the optimization procedure; however, it is always in the defined upper and lower limits. Also, the final SOC is equal to its initial value. The summary for the simulation results of the CEED-RESs problem by considering the RESs as the negative load and the simulation consequences of the CEED-RESs problem by applying the proposed technique are presented in Table II.

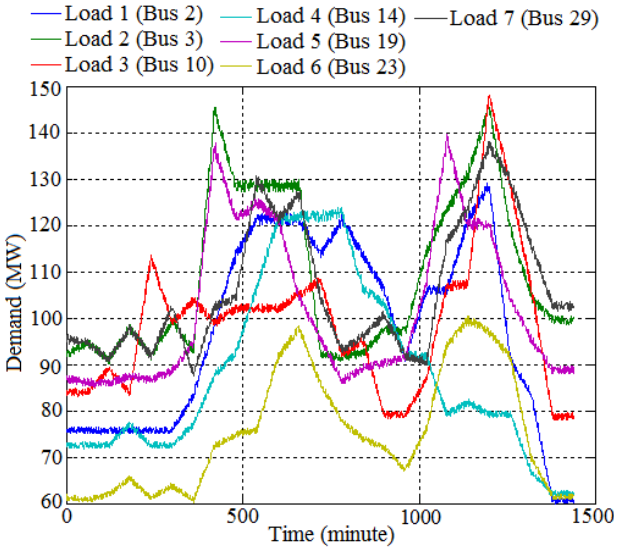

Fig. 6. The predicted demand level at different system buses.

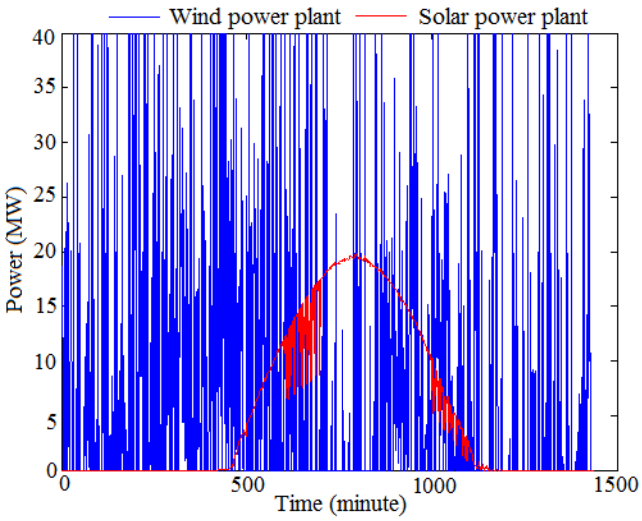

Fig. 7. The value of predicted power of solar and wind power plants installed at bus 4 and 8, respectively.

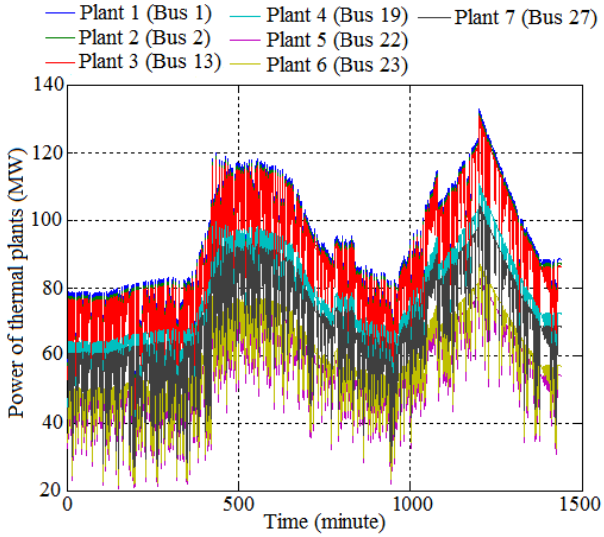

Fig. 8. The generation level of the thermal power plants in CEED problem.

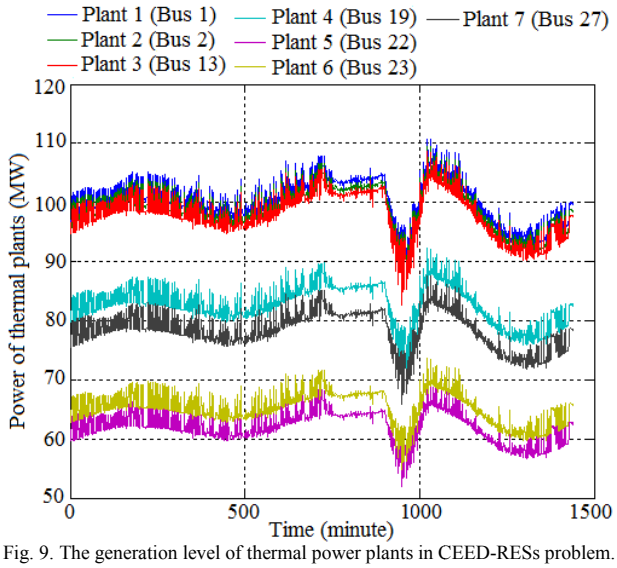

Fig. 9. The generation level of thermal power plants in CEED-RESs problem.

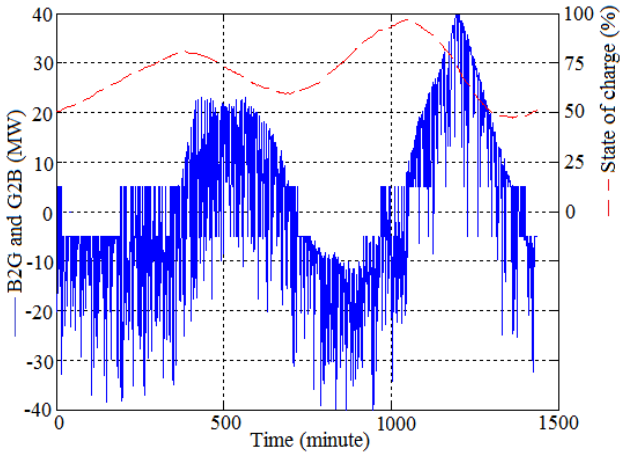

Fig. 10. The generation level and SOC of every battery in CEED-RESs problem.

TABLE II
SIMULATION RESULTS OF THE CEED-RESS PROBLEM UNDER DIFFERENT CASES.

	Emission Level (tons/day)	Operation Cost ($/day)	Emission Saving (tons/day)	Cost Saving ($/day)
CEED-RESs considering RESs as negative load	99,023	2,452,900	-	-
CEED-RESs optimized with the proposed technique	89,859	2,291,700	9,164	161,200

V. CONCLUSION

In this study, a stochastic optimization approach for combined economic and emission dispatch with renewables was presented. Forecasting the uncertain states of the system, modeling uncertainties of the prediction errors, and solving the problem stochastically were the aspects of this new methodology. It was observed that the economic and environmental advantages of the renewables can be maximized via stochastic optimization while satisfying the system security constraints.

REFERENCES

[1]. P. Venkatesh, R. Gnanadass, N. P. Padhy, "Comparison and application of evolutionary programming techniques to combined economic emission dispatch with line flow constraints," *IEEE Trans. Power Syst.,* vol. 18, no. 2, pp. , May 2003.

[2]. M. Huang and Y. C. Huang "A novel approach to real-time economic emission power dispatch," *IEEE Trans. Power Syst.*, vol. 18, no. 1, pp. 288-294, Feb. 2003.

[3]. Y. Xia, S. G. Ghiocel, D. Dotta, D. Shawhan, A. Kindle, and J. H. Chow, "A simultaneous perturbation approach for solving economic dispatch problems with emission, storage, and network constraints," *IEEE Trans. Smart Grid,* vol. 4, no. 4, pp. 2356-2363, Dec. 2013.

[4]. International Energy Agency (IEA) "Energy technology perspectives 2012," *Pathways to a Clean Energy System, Executive Summary,* 2012.

[5]. E. Ela and M. O'Malley, "Studying the variability and uncertainty impacts of variable generation at multiple timescales," *IEEE Trans. Power Syst.*, vol. 27, no. 3, pp. 1324–1333, Aug. 2012.

[6]. E. Ela, V. Diakov, E. Ibanez, and M. Heaney, "Impacts of variability and uncertainty in solar photovoltaic generation at multiple timescales," Nat. Renew. Energy Lab., Golden, CO, USA, Tech. Rep. NREL/TP-5500-58274, May 2013.

[7]. E. Arriagada, E. López, M. López, R. Blasco-Gimenez, C. Roa, and M. Poloujadoff, "A probabilistic economic dispatch model and methodology considering renewable energy, demand and generator uncertainties," *Elect. Power Syst. Res.*, vol. 121, no. 4, pp. 325–332, Apr. 2015.

[8]. G. J. Osorio, J. M. Lujano-Rojas, J. C. O. Matias, J. P. S. Catalao, "A probabilistic approach to solve the economic dispatch problem with intermittent renewable energy sources," *Energy,* vol. 82, no. 3, pp. 949-959, Mar. 2015.

[9]. J. Hetzer, D. C. Yu, and K. Bhattarai, "An economic dispatch model incorporating wind power," IEEE Trans. Energy. Convers. vol. 23, no. 2, pp. 603-611, Jun. 2008.

[10]. S. S. Reddy, P. R. Bijwe, and A. R. Abhyankar "Real-time economic dispatch considering renewable power generation variability and uncertainty over scheduling period" *IEEE Systems Journal*, DOI: 10.1109/JSYST.2014.2325967.

[11]. A. Saber, G. K. Venayagamoorthy, "Plug-in Vehicles and Renewable Energy Sources for Cost and Emission Reductions", *IEEE Transactions on Industrial Electronics*, Vol. 58, No. 4, April 2011, pp. 1229-1238.

[12]. P. Jenkins J. Fletcher, D. Kane, "Lifetime prediction and sizing of lead–acid batteries for micro generation storage applications," *IET Renew. Power Gener.,* vol. 2, no. 3, pp. 191–200, Sep. 2008.

[13]. G. M. Masters, "Renewable and efficient electric power systems," New Jersey, NJ, USA: Wiley, 2004.

[14]. R. H. Liang and J. H. Liao, "A fuzzy-optimization approach for generation scheduling with wind and solar energy systems," IEEE Trans. Power Syst., vol. 22, no. 4, pp. 1665-1674, Nov. 2007.

[15]. S. Pappala, I. Erlich, K. Rohrig, and J. Dobschinski, "A stochastic model for the optimal operation of a wind-thermal power system," *IEEE Trans. Power Syst.,* vol. 24, no. 2, pp. 940-950, May 2009.

[16]. U.S. energy information administration (EIA), [Online]. Available: http://www.eia.gov/tools/faqs/faq.cfm?id=74&t=11, accessed Jan. 2015.

[17]. U.S. energy information administration (EIA), [Online]. Available: http://www.eia.gov/todayinenergy/detail.cfm?id=9310, accessed Jan. 2015.